High-Energy Scale Revival and Giant Kink in the Dispersion of a Cuprate Superconductor

B. P. Xie,[1] K. Yang,[1] D. W. Shen,[1] J. F. Zhao,[1] H. W. Ou,[1] J. Wei,[1] S. Y. Gu,[1] M. Arita,[2] S. Qiao,[2] H. Namatame,[2] M. Taniguchi,[2] N. Kaneko,[3] H. Eisaki,[3] K. D. Tsuei,[4] C. M. Cheng,[4] I. Vobornik,[5] J. Fujii,[5] G. Rossi,[5,6] Z. Q. Yang,[1] and D. L. Feng[1,*]

[1]*Department of Physics, Applied Surface Physics State Key Laboratory, and Advanced Materials Laboratory, Fudan University, Shanghai 200433, China*

[2]*Hiroshima Synchrotron Radiation Center and Graduate School of Science, Hiroshima University, Hiroshima 739-8526, Japan*

[3]*AIST, 1-1-1 Central 2, Umezono, Tsukuba, Ibaraki, 305-8568 Japan*

[4]*National Synchrotron Radiation Research Center and Department of Physics, National Tsing-Hua University, Hsinchu 30077, Taiwan, Republic of China*

[5]*CNR-INFM, TASC Laboratory AREA Science Park–Basovizza, 34012, Trieste, Italy*

[6]*Dipartimento di Fisica, Universitá di Modena e Reggio Emilia, Via Campi 213/A, I-41100 Modena, Italy*

(Received 21 May 2006; published 2 April 2007)

In the present photoemission study of a cuprate superconductor $Bi_{1.74}Pb_{0.38}Sr_{1.88}CuO_{6+\delta}$, we discovered a large scale dispersion of the lowest band, which unexpectedly follows the band structure calculation very well. Similar behavior observed in blue bronze and the Mott insulator $Ca_2CuO_2Cl_2$ suggests that the origin of hopping-dominated dispersion in an overdoped cuprate might be quite complicated. A giant kink in the dispersion is observed, and the complete self-energy containing all interaction information is extracted for a doped cuprate. These results recovered significant missing pieces in our current understanding of the electronic structure of cuprates.

DOI: 10.1103/PhysRevLett.98.147001 PACS numbers: 74.25.Jb, 71.18.+y, 74.72.Hs, 79.60.Bm

The interplay between different energy scales of a physical system usually holds the keys to its various fascinating properties. For cuprate superconductors and their parent Mott insulator, the bandwidth of the so-called Zhang-Rice singlet effective band [1] has been intriguingly illustrated in numerical studies and experiments [2–6] to be $2.2J$ instead of $4t$, J being the magnetic exchange interaction, and t being the hopping integral. This was considered to be an important step toward the ultimate understanding of the high temperature superconductivity [7], which highlights the importance of magnetism. Such an effective band has been widely adopted in various self-energy analyses of the low energy kinks in the cuprate dispersion in terms of either electron-phonon [8–10] or electron-magnon [11,12] interactions. However, the effective bandwidth was based on an extrapolation, since the quasiparticle dispersion in a large region near the Brillouin zone center, Γ, was not identified, possibly due to very broad line shape. From an effective tight binding model [13], hopping parameters could be fitted out of the partial quasiparticle dispersion observed near the Fermi energy E_F. The bandwidth of the occupied part is then extrapolated to be about 0.4 eV [13,14]. Recent technological advances enable us to study electronic structure in a much wider momentum window. It is therefore pertinent to reexamine the ''missing dispersion'' near Γ, and check whether this extrapolation is justified. In this Letter, we report the discovery of such missing dispersion in the photoemission data of a cuprate superconductor $Bi_{1.74}Pb_{0.38}Sr_{1.88}CuO_{6+\delta}$ (Bi2201). We found that sections of coherent and incoherent spectra piece together a full dispersion actually on the order of $4t$ *again*. This large scale dispersion unexpectedly follows the band structure calculation very well, except for a giant kink. These findings provide a fresh picture on the subtle interplay of different energy scales in cuprates. Moreover, the experimental bare band was retrieved, which enables the experimental extraction of the full self-energy of a doped cuprate. So far, only partial self-energy has been studied in most previous experiments. Therefore, the revelation of such a critical quantity that contains the complete interaction information would provide really strong constraints on theory.

Highly overdoped Bi2201 single crystal was prepared by the floating-zone technique and subsequent annealing. The sample's T_c is 5 K, indicating the hole concentration is very close to the superconductor/metal phase boundary. Angle-resolved photoemission spectroscopy (ARPES) data of Bi2201 presented here were measured at the beam line 9 of HiSOR equipped with a Scienta R4000 electron analyzer. The angular resolution is 0.3° and the energy resolution is 10 meV. The data were taken at 20 K with 22.5 eV photons in a 30° angular window. This enables the identification of broad features in momentum distribution curves (MDC's). The samples were aligned by Laue diffraction, and cleaved *in situ* in ultrahigh vacuum better than 5×10^{-11} mbar.

ARPES intensity map of the Bi2201 in a wide energy and momentum range is shown in Fig. 1(a) along the $(0, 0) - (\pi, \pi)$ or nodal direction. Guided by the solid lines, one can clearly observe the band hybridization. The low energy band would have dispersed down to $\sim$1.6 eV below E_F (i.e., $4t$, instead of $2.2J$), if it had not

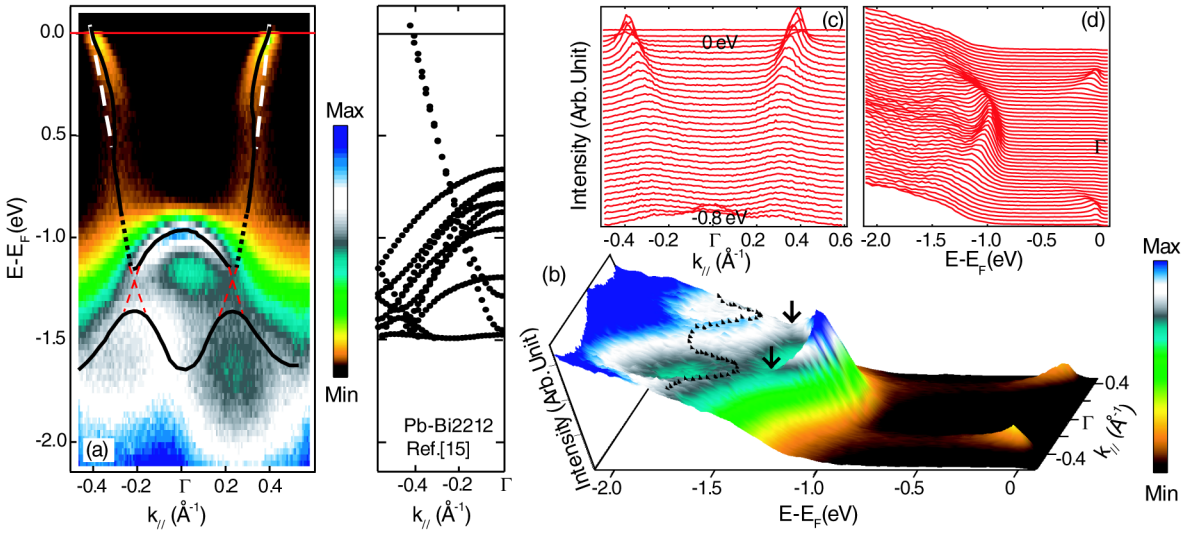

FIG. 1 (color online). Large energy scale dispersion of Bi2201. (a) ARPES intensity map along the nodal direction. The solid lines indicate the experimentally measured dispersion, while the dotted lines are interpolations. The thick dashed lines indicate the linear behavior of the bare band as predicted by LDA calculations. The thin dashed lines illustrate the band crossings. The right side shows the LDA band structure calculated up to 1.5 eV for the nodal direction of Bi2212 from Ref. [15]. (b) The surface plot of the data in (a) to highlight the band crossings (arrows), and high-energy dispersion (black triangles). (c) Selected momentum distribution curves, and (d), energy distribution curves of data plotted in panel (a).

intersected the high-energy bands around -1.2 eV. In the surface plot of the same data [Fig. 1(b)], the two spectral weight dips due to these band intersections are highlighted by the arrows. Moreover, the dispersions in the high-energy region are easily identified here (black triangles). The dispersion within $[-0.9\ \text{eV}, -0.4\ \text{eV}]$ is clearly visible in the MDC's [Fig. 1(c)]. Further experiments at beam line 21B of NSRRC also show that it is robust against the variations of the photon energy and polarization, indicating it is not some matrix element effects. The dispersion and smooth connection to the strong feature near Γ confirm that it is not caused by some secondary electron background. Therefore, the strong feature around Γ is part of the same band as the quasiparticle band near E_F. On the other hand, their relation is not obvious in the energy distribution curves (EDC's) in Fig. 1(d), where the dispersion within $[-0.9\ \text{eV}, -0.4\ \text{eV}]$ cannot be resolved. The band and dispersion energy scales identified in Fig. 1(a) agree with the recent local density functional (LDA) band structure calculation of the Pb-doped bilayer $Bi_2Sr_2CaCu_2O_{8+\delta}$ compound very well [right side of Fig. 1(a)] [15], as the bilayer splitting is minimal along the nodal direction [16]. The strong quasiparticle peak near Γ is shown mostly to be consisting of other Cu d and O p orbitals than those for the band close to E_F. The well-preserved quasiparticles at such high energies [Fig. 1(d)] indicate correlation effects are quite weak for these orbitals. So far, we have revealed an anomalous electronic structure for Bi2201: well-defined coherent quasiparticles exist at both high energies and low energies, giving a total occupied band width of 1.2 eV, while broad features that follow the bare band dispersion dominate the intermediate energy region. In particular, the experimental dispersion near E_F deviates from the straight line in the band calculation, and exhibits a large kink.

This wide dispersion exists over a large region of the Brillouin zone. As shown in Fig. 2, besides the nodal cut in Fig. 2(a), it is also observed in cuts #2 and #3, which is halfway between the nodal and antinodal regions. In cuts #4 and #5, the renormalized band is located near E_F. A weak feature also exists at high energy, although there is no missing band dispersion. However, compared with cuts #1–#3, the high-energy feature in cuts #4 and #5 is weaker, extends straight into high energies, and does not show a connection with the high-energy band. On the other hand, the broad line shape and the resemblance do suggest the high-energy features observed in cuts #1–#3 contain significant incoherent weight. Recently, high-energy dispersion beyond the $2.2J$ and incoherent line shape in the Mott insulator $Ca_2CuO_2Cl_2$ were reported [17], which have also been observed in various numerical studies of hole motion in an antiferromagnetic spin background [4,18,19]. However, the hole concentration of the heavily overdoped system under study is about $1/4$, so that antiferromagnetic order no long exists, and even long range spin fluctuations diminish as observed in inelastic neutron scattering measurements [20]. Therefore, the effects of the spin degree of freedom are not obvious here.

The other known precedent of similar behavior was observed in the 1D charge density wave system blue bronze. Figure 3 shows the photoemission data of blue bronze. The broad spectrum in Fig. 3(a) was attributed to

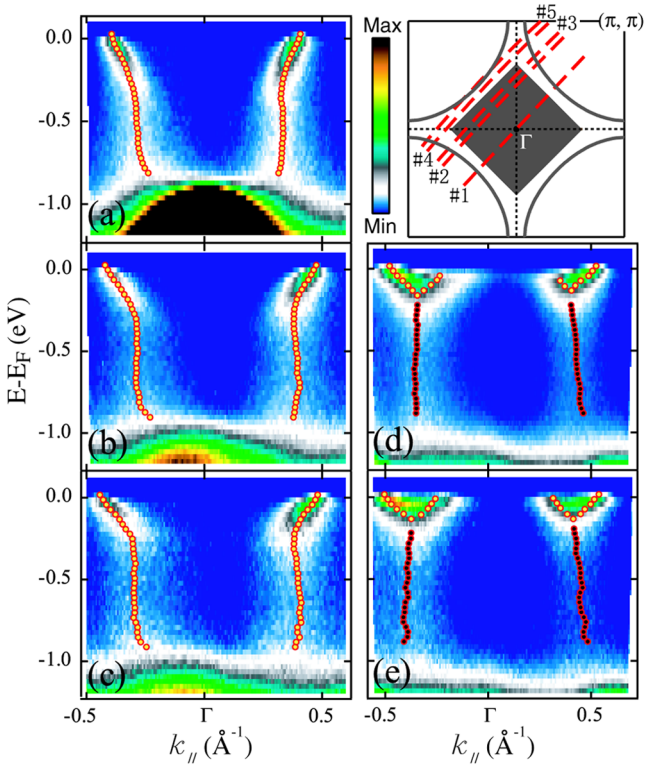

FIG. 2 (color online). Momentum dependence of the high-energy dispersion. (a)–(e) Photoemission intensity taken along the cuts #1–#5, respectively, as illustrated in the inset on the top right corner, where large energy scale dispersion happens in the dark region. The light dots mark the position of the measured band dispersion, while the black dots in (d) and (e) indicate the centroid of the incoherent feature.

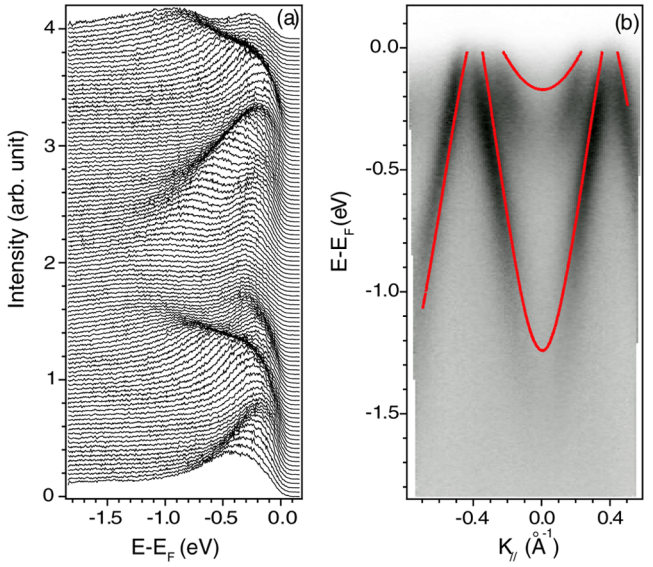

FIG. 3 (color online). (a) ARPES spectra of $K_{0.25}Rb_{0.05}MoO_3$ along the chain direction. Data were taken at normal state ($T = 210$ K) at the APE beam line of ELETTRA. (b) ARPES intensity map for the data in (a). The thick lines are the bare band structure from LDA calculations [25].

the incoherent multiple phonon excitations in this polaronic system, while the quasiparticles are renormalized to the vicinity of E_F with diminishing weight [21]. Yet, these incoherent features exhibit clear dispersion and well follow the calculated band structure [solid curves in Fig. 3(b)]. Theoretically, it has been shown in the strong electron-phonon coupling regime that the incoherent broad features reflect the local hoppings of electrons in various frozen lattice configurations, and thus follow the bare band structure dispersion [22]. Considering the small carrier density in cuprates, screening for electron-phonon interactions is weak; plus the low energy kink structure in the dispersion of cuprate was clearly observed across the entire doping range, and was arguably related to electron-phonon interactions [14,23]. Therefore, it is not unreasonable to speculate that electron-phonon interactions may play an important role in the large scale dispersion observed here, although it may not be the sole cause.

The remarkable giant kink structure observed in Figs. 1 and 2 and the linear dispersion behavior near E_F predicted by LDA calculations provide a rare chance to extract the full self-energy Σ of a strongly correlated system, which reflect *all* correlation effects in the system. Figure 4(a) shows the real part of the self-energy Σ', which is the difference between the measured band and the bare band. Here, the bare band, e.g., the thick dashed line in Fig. 1(a), is the extrapolation of the linear dispersion at higher energies as suggested by the LDA calculation, which goes through the Fermi crossing so that Σ' naturally vanishes at $\omega = 0$. In previous studies, because of the lack of bare band information, a fraction of the self-energy, Σ'_{eff}, was retrieved by assuming a local effective band structure [23]. The resulting partial self-energy was argued to contain information on interactions between electrons and certain bosons. As shown in Fig. 4(a), Σ'_{eff} is only a small fraction of Σ'. Away from the nodal cut, Σ' increases toward the antinodal direction. Interestingly, as shown in the inset of Fig. 4(a), Σ' of different cuts can be scaled to a universal curve, where even the details of the low energy kink structures match each other. These raise the questions of whether the low energy kink is just a part of a large scale structure, and whether the kink extracted in conventional analysis cleanly represents the interaction between electrons and bosons [8–12]. The $Ca_2CuO_2Cl_2$ data are also plotted in Fig. 4(a) for comparison [17].

The imaginary part of the self-energy Σ'' is shown in Fig. 4(b), which is the product of the MDC width and the bare band velocity [the slope of the thick dashed line in Fig. 1(a)]. Generally, it increases rapidly in the first 0.35 eV, then gradually saturates at high binding energies. For comparison, Σ''_{KK}, the Kramers-Kronig transformation of Σ', is shown here [24]. Within the first 250 meV below E_F, a quasiparticle peak could be observed in the EDC's, the good agreement between Σ'' and Σ''_{KK} on the low

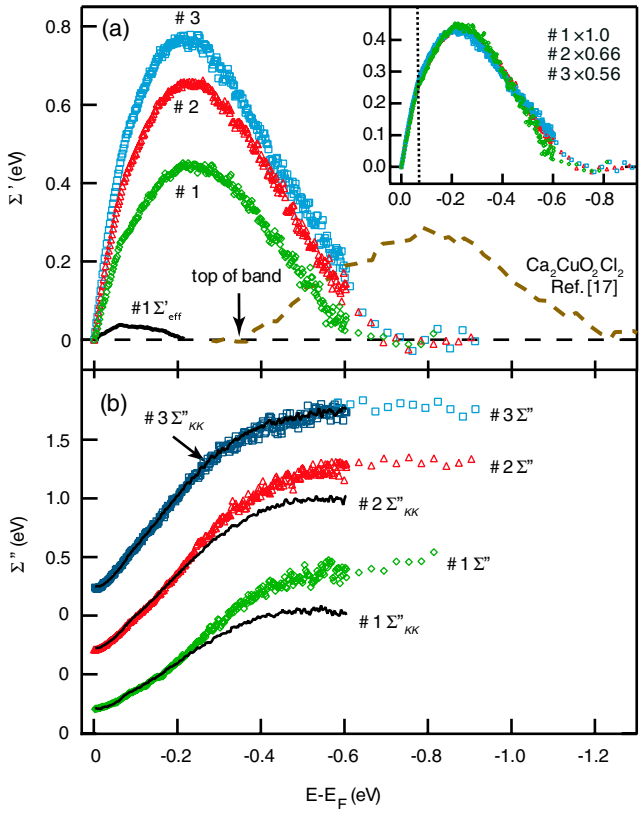

FIG. 4 (color online). Self-energy of the Bi2201. (a) Σ' for cuts #1 (diamonds), #2 (triangles), and #3 (squares). The solid line is Σ'_{eff}. The dashed line is the high-energy kink observed in parent Mott-insulator compound $Ca_2CuO_2Cl_2$ for comparison purpose [17], the arrow marks the top of its band. Inset: The Σ' for cuts #1–#3 could be rescaled to match each other, where the dashed line indicates the low energy kink position. (b) Σ'' for cuts #1–#3 are stacked. The solid curves are the Σ''_{KK}.

energy side for all three cuts confirms that the full self-energy has been reliably extracted at least in this range, where one could define the quasiparticles. On the other hand, the deviation at high energies may reflect the interesting incoherent nature of the electronic structure there. We note that the large amplitude and energy expansion of Σ at such high doping is quite anomalous, which indicates possibly some critical ingredients were missing or underestimated in our previous understanding of the cuprate. The self-energy measured here provides direct and critical information for the development of theory for cuprates. Moreover, the observations of large energy scale dispersion of the incoherent features in both the antiferromagnetic Mott insulator and the heavily overdoped system illustrate the complexity of the problem.

To summarize, we have presented a global picture of the electronic structure in a highly overdoped cuprate. Contrary to previous perceptions, although the low energy quasiparticles exist in the J energy scale, an incoherent spectral feature disperses on the order of several t, which is analogous with what is observed in the blue bronze. Moreover, various intriguing new information is revealed under this global picture, such as the much larger amplitude and energy expansion of the giant kink compared with the low energy kink discussed before, the universal scaling of Σ', and resemblance to the insulator. Since the high-energy and local physics set the footing for low energy properties, these findings put strong constraints on models that are designed to understand high temperature superconductivity in a realistic cuprate material.

D. L. F. would like to thank Professor Z. Y. Weng and Professor J. P. Hu for helpful discussions. This work was supported by NSFC, STCSM, the 973 project (No. 2006CB601002, No. 2006CB921300) of The Ministry of Science and Technology of the People's Republic of China (MOST), and ITCP-ELETTRA project.

*Electronic address: dlfeng@fudan.edu.cn

[1] F. C. Zhang and T. M. Rice, Phys. Rev. B **37**, 3759 (1988).
[2] B. O. Wells *et al.*, Phys. Rev. Lett. **74**, 964 (1995).
[3] F. Ronning *et al.*, Science **282**, 2067 (1998).
[4] C. Dahnken, M. Aichhorn, W. Hanke, E. Arrigoni, and M. Potthoff, Phys. Rev. B **70**, 245110 (2004).
[5] E. Dagotto, R. Joynt, A. Moreo, S. Bacci, and E. Gagliano, Phys. Rev. B **41**, 9049 (1990).
[6] T. Tohyama, Phys. Rev. B **70**, 174517 (2004).
[7] Z. X. Shen and G. A. Sawatzky, Phys. Status Solidi (b) **215**, 523 (1999).
[8] T. Cuk *et al.*, Phys. Rev. Lett. **93**, 117003 (2004).
[9] X. J. Zhou *et al.*, Phys. Rev. Lett. **95**, 117001 (2005).
[10] A. Lanzara *et al.*, Nature (London) **412**, 510 (2001).
[11] P. D. Johnson *et al.*, Phys. Rev. Lett. **87**, 177007 (2001).
[12] T. Valla, Proc. SPIE Int. Soc. Opt. Eng. **5932**, 593203 (2005).
[13] M. R. Norman, M. Randeria, H. Ding, and J. C. Campuzano, Phys. Rev. B **52**, 615 (1995).
[14] K. Yang *et al.*, Phys. Rev. B **73**, 144507 (2006).
[15] H. Lin, S. Sahrakorpi, R. S. Markiewicz, and A. Bansil, Phys. Rev. Lett. **96**, 097001 (2006).
[16] D. L. Feng *et al.*, Phys. Rev. Lett. **86**, 5550 (2001).
[17] F. Ronning *et al.*, Phys. Rev. B **71**, 094518 (2005).
[18] C. Grober, R. Eder, and W. Hanke, Phys. Rev. B **62**, 4336 (2000).
[19] Z. Y. Weng, V. N. Muthukumar, D. N. Sheng, and C. S. Ting, Phys. Rev. B **63**, 075102 (2001).
[20] S. Wakimoto *et al.*, Phys. Rev. Lett. **92**, 217004 (2004).
[21] M. Grioni, L. Perfetti, and H. Berger, J. Electron Spectrosc. Relat. Phenom. **137**, 417 (2004).
[22] O. Rösch and O. Gunnarsson, Eur. Phys. J. B **43**, 11 (2005).
[23] X. J. Zhou, T. Cuk, T. Devereaux, N. Nagaosa, and Z. X. Shen, cond-mat/0604284.
[24] There are some model dependence for the calculated Σ''_{KK} on the high-energy side; however, we emphasize that the results below 0.35 eV binding energy are robust against these numerical details as shown by A. A. Kordyuk *et al.*, Phys. Rev. B **71**, 214513 (2005).
[25] José-Luis Mozos *et al.*, Phys. Rev. B **65**, 233105 (2002).